Available online at www.sciencedirect.com
ScienceDirect
Trans. Nonferrous Met. Soc. China 21(2011) 717−724
Transactions of Nonferrous Metals Society of China
www.tnmsc.cn

Effect of inclusion on service properties of GW103K magnesium alloy

LIANG Min-jie[1, 2], WU Guo-hua[1], DING Wen-jiang[1], WANG Wei[1]

1. School of Materials Science and Engineering, Shanghai Jiao Tong University, Shanghai 200240, China;
2. School of Materials Science and Engineering, North University of China, Taiyuan 030051, China

Received 25 September 2010; accepted 25 December 2010

Abstract: The effects of inclusions on microstructure, mechanical property, corrosion behavior of Mg-10Gd-3Y (GW103K) alloys by unrefining, MgO ceramic filtering and JDMJ flux refining were investigated, respectively. The results indicate that with decreasing significantly the number and size grade of inclusions for the alloy refined with JDMJ flux, tensile strength and elongation increase; however, the yield strength is less than that of the alloy refined with MgO ceramic filter and unrefined alloy. With the decrease of the inclusions contents, the corrosion rate of the alloys quickly vary from 2.419 mg/(cm^2·d) to 1.265 mg/(cm^2·d). After inclusion content is reduced to 0.385%, the corrosion rate has almost no changes. Finally, the relationship between the volume fraction of inclusions and service properties of GW103K alloy under different conditions are established quantitatively.
Key words: Mg-10Gd-3Y alloy; inclusion; purification; service properties

1 Introduction

Due to the unique advantages of high-strength, heat and corrosion resistance, rare-earth magnesium alloys have broader application prospects in defense, industrial production than conventional magnesium alloys[1−2]. A lot of researches have been focused on magnesium alloy containing heavy rare-earth elements, such as Mg-Gd alloys. Many results related to the microstructure and mechanical properties of Mg-Gd-Y-Zr alloy have been reported[1−3], and interest in their application is still increasing. Although the alloy systems show high strength, the presence of inclusion is still one of the important bottlenecks to its rapid development.

It is known that the inclusion has an important influence on material properties, such as strength, toughness, fatigue resistance, fluidity and casting performance, and corrosion resistance[4−10]. So far, the evaluation system of aluminum and steel inclusion has been established, while the magnesium alloy in this domain is still in its early stages[6]. Especially, there is no clear criteria for quantitative and qualitative analysis methods, testing and evaluation methods of inclusion and inclusion control level, etc. Therefore, the study on inclusions for further improving the inherent quality of magnesium alloy has practical significance.

In recent years, the inclusion researches in the magnesium alloy heve attracted more and more attention. ZHANG et al[11] studied the sedimentation rules of the inclusion for the magnesium alloy. ZHANG et al[12] investigated the compositions and morphology of MgO inclusion particle in AZ91 magnesium alloy. ZHAO et al[13] analyzed the formation process of inclusions and the effect on the quality of AZ91D magnesium alloy. Despite the above interesting findings, there is still a lack of research on the rare-earth magnesium alloy.

For Mg-Gd-Y-Zr alloy, the current studies are mainly focused on the purification process and means, while the information of existed inclusions in morphology, size, distribution, quantity and other quantitative analysis is still very scarce. Moreover, the researches on the relationship between the inclusion and the service properties of materials are still not reported for Mg-Gd-Y-Zr system.

In order to display the intrinsic relationship between the inclusions and material service properties, the present research is to discuss the effect of inclusions on the microstructure, mechanical property, corrosion behavior of Mg-10Gd-3Y-0.5Zr (GW103K) alloy.

Foundation item: Project (2007CB613701) supported by the National Basic Research Program of China; Project (20100470125) by National Science Foundation for Post-doctoral Scientists of China; Project (2009021028) supported by Science and Technique Foundation for Young Scholars of Shanxi Province, China
Corresponding author: LIANG Min-jie; Tel: +86-13621759370; Fax: +86-21-34202794; E-mail: lmj2005686@sina.com
DOI: 10.1016/S1003-6326(11)60771-1

2 Experimental

2.1 Materials

GW103K alloy was fabricated with high purity Mg (99.95%, mass fraction, the same below if not mensioned), Mg-25Gd, Mg-25Y and Mg-30Zr master alloys in an electrical resistance furnace under a mixed protective gas of CO_2 and SF_6 in the volume ratio of 100:1. The JDMJ flux ($MgCl_2$ 45, KCl 25, NaCl 20, others 10) developed by Shanghai Jiao Tong University, was added into the melt for removing the inclusion.

2.2 Procedure

Mg and other alloy materials, JDMJ fluxes and tools used in the experiments were heated to 200 °C in a baking oven before experiment in order to eliminate water. Smelting was performed in a 7 kW-crucible electric resistance furnace under protective gas atmosphere. The partial melt alloy was poured at 740 °C before flux refining, and then JDMJ flux was added to refine the remainder melt at 760 °C. After refining, the residual melt was held for 30–45 min, and then at 740 °C it was poured into the metallic molds preheated to 400 °C. Metallographs and morphologies of the alloy were observed with optical and scanning electron microscope. The compositions of inclusions were analyzed with energy dispersive spectroscope (EDS) attached to the SEM. Using the OLYMPUSPME3 and Leco image software, the quantity and the size of inclusion were tested for the specimen.

Tensile test samples were cut into rectangular specimens with dimensions of 10 mm in width, 2 mm in thickness and 25 mm in gauge length by an electric-sparking wire-cutting machine. Tensile testing was carried out on a Zwick/Roell−20kN material test machine at a cross head speed of 0.5 mm/min at room temperature.

The dimensions of specimens for immersion corrosion test were 35 mm × 4 mm. The immersion tests were conducted by immersing the specimens in 5% NaCl solution at 25 °C for 72 h, which were prepared with analytical reagent grade NaCl and distilled water. After 3 d immersion, the specimens were cleaned by dipping in a solution of 15% Cr_2O_3 + 1% $AgNO_3$ (volume fraction) in 500 mL water under boiling condition for about 5 min. The corrosion rates were obtained (in mg/(cm^2·d)).

Electrochemical polarization tests were carried out in 5% NaCl solution saturated with $Mg(OH)_2$ using a PARSTAT 2273 advanced electrochemical system. Open circuit potentials (EOC), polarization curves and electrochemical impedance spectroscopy (EIS) of the specimens were measured. For all measurements, a three-electrode electrochemical cell was used, with a saturated calomel electrode (SCE) as a reference electrode and a high-density graphite electrode as the counter. Specimens were immersed in the test solution and a polarization scan was carried out at a rate of 1 mV/s, allowing a steady state potential to develop.

3 Results and discussion

3.1 Morphologies of inclusion

Since the chemical properties of magnesium are very active, the production of the original magnesium, magnesium alloy smelting and processing will inevitably bring many inclusions, while the main types of inclusions have the non-metallic, metal and gas inclusions. Through SEM and EDS analysis for many view fields of specimens, it is indicated that the inclusions are mainly non-metallic inclusions, that is, Mg, Gd and Y oxides inclusions; meanwhile, MgO inclusions with different morphologies and sizes are perfectly dominant, which account for more than 85%. Figure 1 shows the typical SEM images for MgO inclusions with different morphologies.

Figure 2 shows the microstructures of GW103K alloys unrefined, MgO filtered and JDMJ flux refined, respectively. It can be seen that a large amount of block and fine inclusions particles distribute in the unrefined GW103K alloy. Compared with Fig.2(a), after MgO filtering the large inclusion particles disappeared, but there were still many fine inclusions in the alloy. Meanwhile, in the alloy purified by JDMJ flux, the number of inclusions reduced significantly, and only few of cluster and fine inclusion particles appeared. Alloy melt was relatively clean and the grain boundaries seemed to be much cleaner. From the image, it can be seen that purification methods do not impact on the composition of phase in this alloys. The XRD diffraction analysis indicated that the phase compositions of the alloys purified by the different manners have almost no changes and still consist of α-Mg phase and $Mg_{24}(GdY)_5$ eutectic phase[14].

Therefore, it may be believed that inclusion, which affects the alloy properties, is mainly one of the factors. In order to further reveal the interrelation between the inclusions and the alloy properties, it is necessary to analyze quantitatively the volume fraction and size of inclusions in the alloy purified with different methods. In this work, the inclusion content was calculated using general quantitative metallographic method, which was carried out through the average volume fraction of inclusions in the different visual fields.

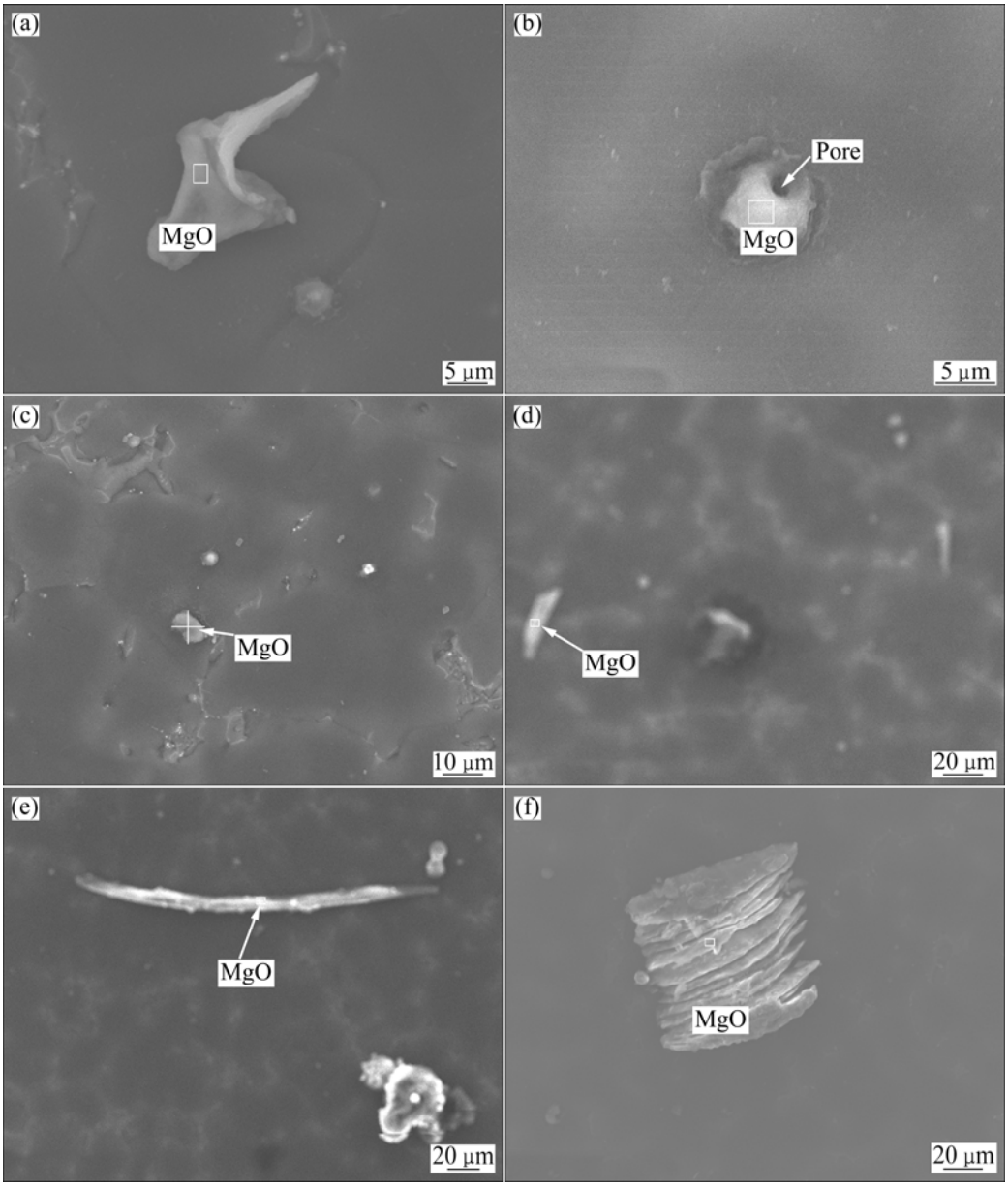

Fig.1 SEM images of MgO inclusions: (a) Z-shaped MgO; (b) Spherical MgO; (c) Block MgO; (d) Rod-like MgO; (e) Needle-like MgO; (f) Lamellar MgO

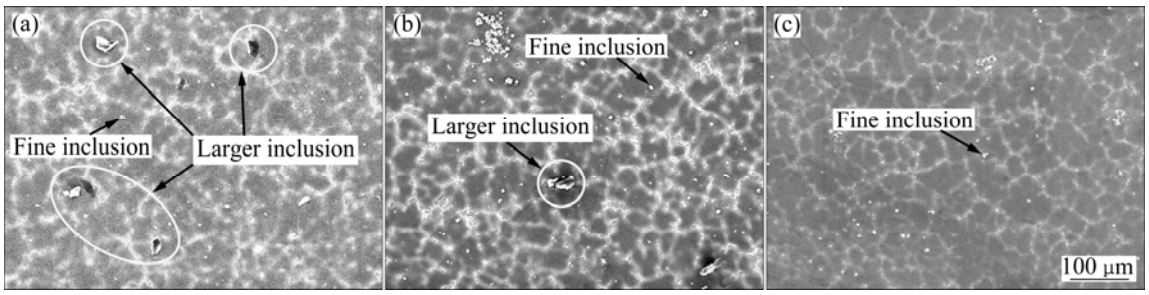

Fig.2 Microstructures of GW103K alloy refined by different methods: (a) Unrefined; (b) MgO filtered; (c) JDMJ flux refined

In order to determine the quantities of inclusions, the contents and sizes of inclusions in GW103K alloys were calculated for 30 view fields using Leco image software with an optical microscope (OM, OLYMPUS PME3). The volume fractions and size grades of inclusions in GW103K alloys are shown in Fig.3 and Table 1. It can be seen that the inclusions with the diameter of 1−10 μm (2−4 grades) are dominate, and the

amount of the larger inclusion particles reduce significantly with gradually increasing the inclusion size. The number of inclusions with the diameter of 15−20 μm (the 6th grade) is the least. This indicates that the small size inclusions with the diameter of 1−10 μm are not sensitive to MgO filter, but the number of inclusions with the diameter in the 5th−7th grades is reduced significantly. The total inclusions contents in the alloy by JDMJ flux purified are decreased obviously, especially the inclusions of 15−20 μm almost disappear.

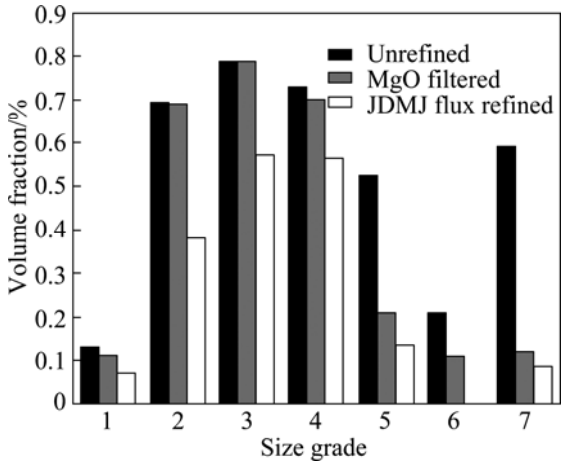

Fig.3 Volume fraction and size grade of inclusions in GW103K alloys unrefined, MgO filtered and JDMJ flux refined, respectively

Table 1 Size grade of inclusions

Size grade	1	2	3	4	5	6	7
Size/μm	<1	1−2	2−5	5−10	10−15	15−20	>20

3.2 Effect of inclusions on mechanical properties

Figure 4 shows the effects of inclusions on mechanical properties of GW103K alloy with different purifying methods. Compared with the unrefined specimens, the ultimate tensile strength (σ_b) and the elongation (δ) increase, which are 196.67 MPa and 1.15% to peak value 205.12 MPa and 3.026%, respectively. Moreover, the elongation of the alloy refined by JDMJ flux is improved significantly. The elongation attains the highest value, 3.026% of the alloy refined by JDMJ flux. However, for the unrefined specimen and specimen with MgO filtered, the elongations are only 1.15% and 1.74%, respectively. The yield strength (σ_s) declines slightly for the alloy refined by JDMJ flux, while for the unrefined specimens, the σ_s reaches 153.2 MPa, which is lower than that of the only MgO filtered specimen and still higher than that of pure JDMJ flux refined specimens.

It is notable that the larger inclusions are removed from the alloy refined by MgO filter, but there still are a substantial number of small particles, which play a dispersion strengthened role. Therefore, the yield strength of this alloy is higher than that of the alloy refined by JDMJ flux. At the same time, in the alloy not only the large inclusion particles but also the fine inclusion particles can be almost removed after using JDMJ flux, which reduces the microcracks source and improves the tensile strength.

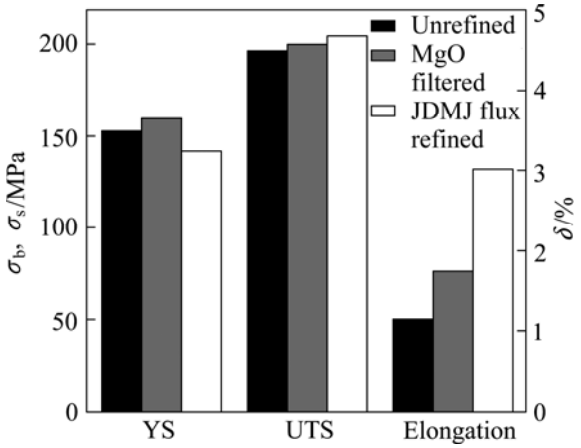

Fig.4 Effects of purifying treatments on mechanical properties of GW103K alloy

From the above results, it may be concluded that the reduction of inclusions, especially the decrease of large inclusion particles could improve significantly the mechanical properties of the alloy and make it present more ductility. The larger inclusions are more likely to destroy the continuity of magnesium matrix, and lead to the stress concentration and supply flaw source. In specially, there are general many microscopic holes around the non-metallic inclusions, that is, the coexistence of inclusion and gas. From Fig.5, It can be seen that the pores adhere to the inclusion from TEM image. Generally, the larger inclusions present the morphology of loose clusters and adhere to the pore, which may become directly the crack source so that the material intensity is reduced greatly.

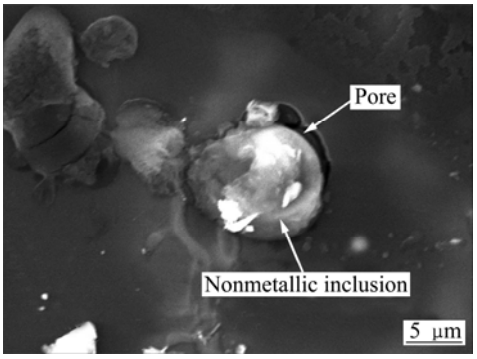

Fig.5 Pores adhered to nonmetallic inclusions in GW103K alloy

Consequently, the micro-voids maybe come into being preferentially in the larger inclusions or at the interfaces. During deformation, cracks emerge and develop into micro-holes gradually as the adjacent holes are interconnected one another, which finally leads to the fracture and thus damage the mechanical properties.

On the other hand, the existences of small inclusions particles do not completely bring to the disadvantages to the alloy. From the TEM image in Fig.6, it can be seen the relationship between the fine nonmetallic inclusion and dislocations. A certain number of fine inclusions distributed in the alloy cause the dislocation pile-up, which could probably hinder the dislocation gliding, thus the yield strength of the alloy could be improved to some extent.

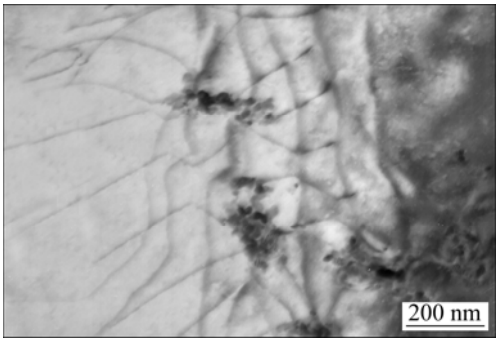

Fig.6 Nonmetallic inclusion and dislocation in alloy

Considering the effectiveness of inclusion content, the relationship between the volume fractions(φ) of the inclusions and mechanical properties is present in Fig.7 for GW103K alloy.

3.3 Effect of inclusion on corrosion properties

3.3.1 Morphology and corrosion rate

Figure 8 shows the morphological characteristics of the corroded surfaces of GW103K alloy in 5% NaCl solution. It can be seen that specimen refined by JDMJ flux has almost no corroded area, except some corrosion pits. The localized corrosion area on the specimen of MgO filtered is obviously less and the corrosion pits become sparser and shallower than that on the unrefined specimen.

The corrosion rates of GW103K alloys unrefined, MgO filtered and pure JDMJ flux refined after immersion in 5% NaCl solution for 3 d are shown in Fig.9(a). The corrosion rates of GWl03K decrease in the

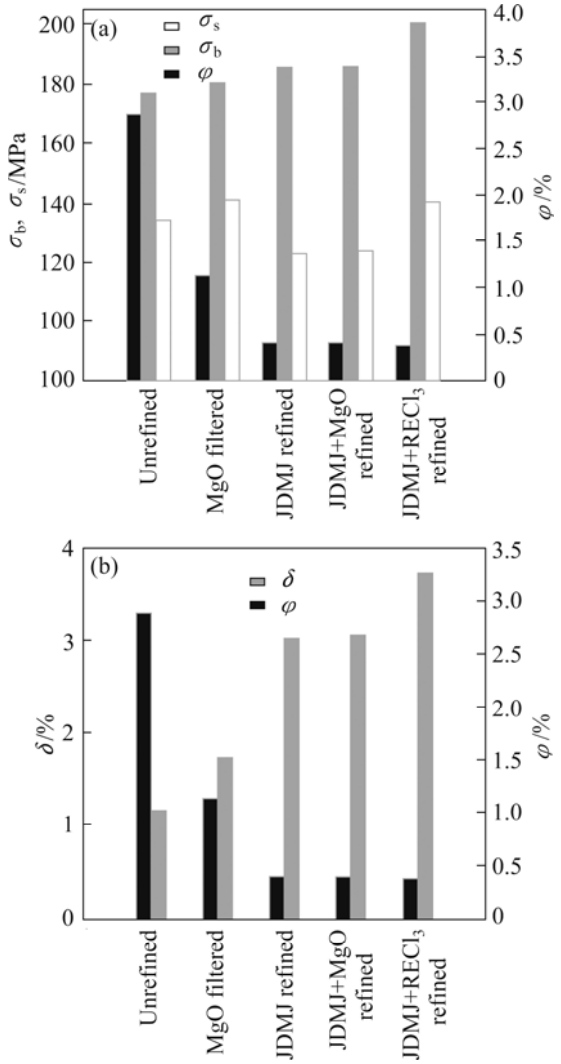

Fig.7 Relationships between volume fractions of inclusions and strength (a), elongation (b) of GW103K alloy under different conditions

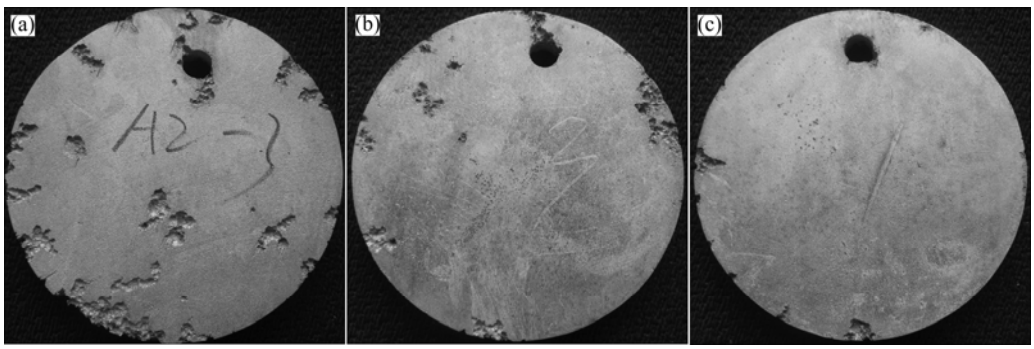

Fig.8 Morphological characteristics of corroded surfaces of GW103K alloy in 5% NaCl solution under three different conditions: (a) Unrefined; (b) MgO filtered; (c) JDMJ flux refined

following order: unrefined >MgO filtered > JDMJ flux refined. Compared with the unrefined alloy, the corrosion rates of these alloys decrease quickly from 2.419 mg/(cm^2·d) to 1.265 mg/(cm^2·d), the corrosion rates of the alloy refined by JDMJ flux is only about half of that of the unrefined alloy, and the corrosion rate of the alloy refined by MgO filter also decreases obviously. In order to further reveal the effect of the inclusions on the corrosion behaviors of the alloy, the relationships between the corrosion rates and inclusion contents are illustrated in Fig.9(b). From the above results, it is indicated that corrosion rates of alloy reduce with decreasing the inclusion content; however, when the amount of inclusions is reduced to certain content (0.385%) and then the corrosion rate almost has no obvious change. This shows that there is a reasonably close correlation between inclusion content and corrosion rate for this alloy.

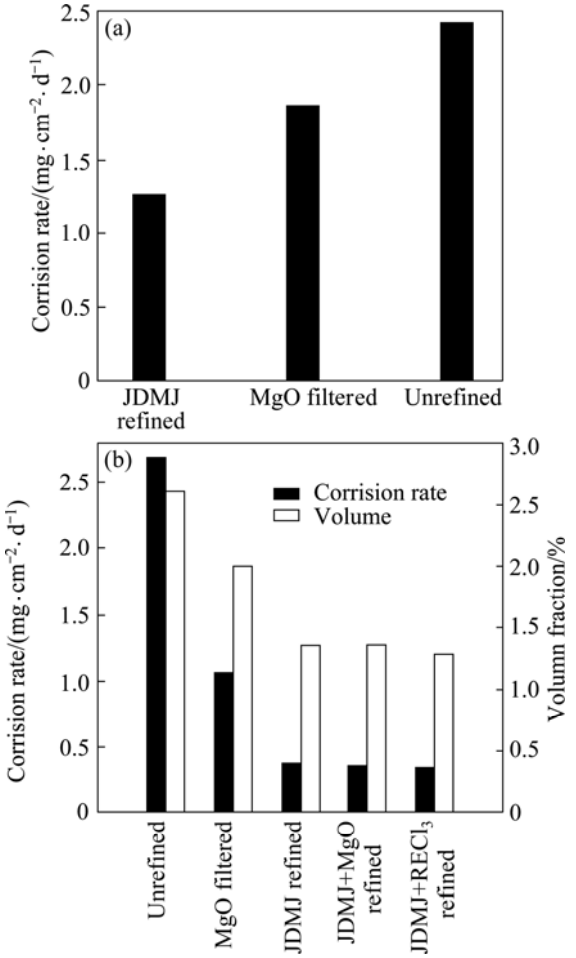

Fig.9 Corrosion rates of GW103K alloy after immersion in 5% NaCl solution for 3 d (a) and relationship between volume fractions of inclusions and corrosion rates of alloy (b)

3.3.2 Electrochemical behaviour

1) Potentiodynamic polarization. The potentiodynamic polarization curves of GW103K alloy containing different inclusion contents in 5% NaCl solution saturated with $Mg(OH)_2$ are present in Fig.10. Generally, the cathodic polarization curves are assumed to represent the cathodic hydrogen evolution through water reduction, while the anodic ones represent the dissolution of magnesium[15]. Figure 10 shows the corrosion potential (φ_{corr}) and corrosion current density (J_{corr}) of GW103K alloy with unrefined, MgO filtered and JDMJ flux refined, respectively. It is found that the polarization curves for all the specimens are not symmetrical between their anodic and cathodic branches. The anodic polarization branches present more obvious changes in lg$J$ versus applied potential than the cathodic polarization branches. And it can be seen that the corrosion potential of unrefined alloy is obviously lower than that of the alloy MgO filtered and JDMJ flux refined in turn. Moreover, the cathodic current density is higher for specimen refined by JDMJ than unrefined alloy potential. This reveals that the cathodic reaction is easier kinetically for the specimen unrefined than the other two ones, which maybe owing to the existence of the different inclusion contents in this alloy. Compariing the GW103K alloys under three conditions shows that the decrease of inclusion contents leads to an increase in φ_{corr} and J_{corr}.

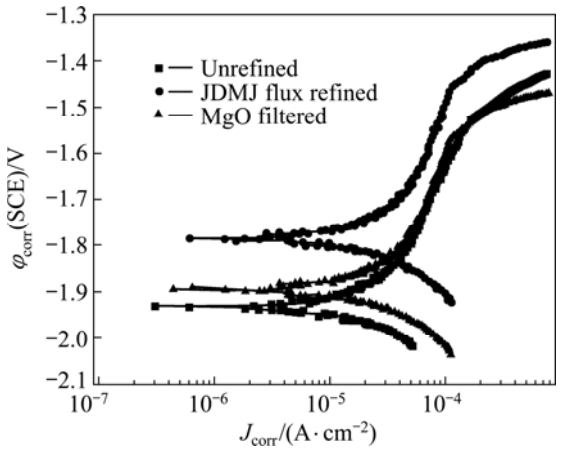

Fig.10 Polarization curves of GW103K alloy under three different conditions

2) Electrochemical impedance spectroscopy (EIS). EIS measurement is an effective method to analyze the alloy corrosion behaviors. The EIS results of GW103K alloy under three conditions are presented in Fig.11. For all the alloys, the characteristics of their EIS spectra are similar except for the difference in the diameter of the loops. This means that the corrosion mechanisms of the specimens are the same, but their corrosion rates are different. Some researchers have indicated that the higher frequency (HF) loop has the better corrosion resistance. From Fig.11, it can be seen that the HF semi-circuit loops increase in the order as follows:

2 163.8 Ω·cm^2 (unrefined) < 2 410.69 Ω·cm^2 (MgO filtered) <3 279.78 Ω·cm^2 (JDMJ flux refined), that is to say, the corrosion resistance of the alloy is obviously improved with the decrease of the inclusions from 2.87% to 0.385%. The relationship between the inclusion and EIS is listed in Table 2. Combined with the results of potentiodynamic polarization and EIS, it is in agreement with the results of immersion tests (Fig.9).

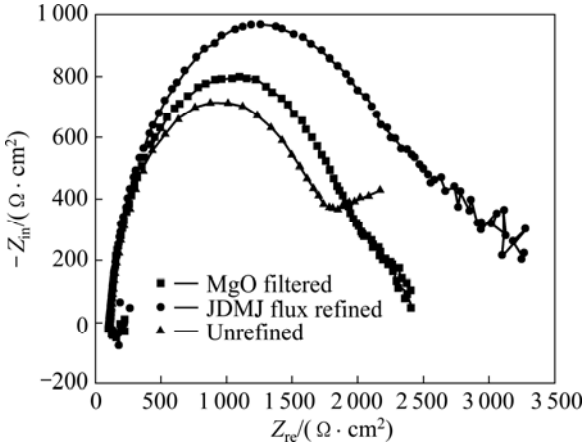

Fig.11 Electrochemical impedance spectroscopy (EIS) results of GW103K alloys under three different conditions

Table 2 Relationship between electrochemical properties and inclusion contents

Refining method	φ_{corr}(SCE)/V	Z_{re}/(Ω·cm^2)	Volume fraction/%		
			Max	Min	Average
Unrefined	−1.932	2 163.8	5.90	0.130	2.870
MgO filtered	−1.891	2 410.69	2.10	0.098	1.120
JDMJ refined	−1.786	3 279.78	0.86	0.070	0.385

Consequently, from the above results, it can be seen the difference in corrosion resistance of GW103K alloy under different conditions (Table 2), which is owing to the content of the inclusions, so that leads to the great influence on the corrosion resistance of GW103K alloy. Further analysis from relationship between inclusions and the corrosion mechanism, it may be explained the reason of the existing electronegativity differences between inclusions and magnesium matrix. The inclusions act as cathode and form galvanic coupling corrosion with the Mg matrix, the deleterious of inclusions on corrosion resistance of magnesium alloys can be attributed to the forming of galvanic coupling, which accelerates the corrosion process of the alloy. On the other hand, owing to the inclusions acting as cathode in galvanic coupling corrosion, the reduction of inclusions content will lead to the cathode areas decreasing and thus improve the corrosion resistance of the alloy.

4 Conclusions

1) The content and size of inclusions have great influence on the mechanical properties, while the size effect of inclusions is not sensitive to the corrosion resistance.

2) The decrease of large inclusion could improve significantly tensile strength (σ_b) and make the alloy present the high elongation (δ). However, a certain number of fine inclusions, which could probably act as obstacle dislocation gliding, can improve the yield strength of the alloy.

3) The reduction of inclusion content will lead to the cathode areas decreasing with galvanic coupling corrosion and thus improve obviously the corrosion resistance of the alloy, but when the content of inclusion is less than 0.385%, inclusions have no obvious influence on corrosion properties.

References

[1] NIE J F, GAO X，ZHU S M. Enhanced age hardening response and creep resistance of Mg-Gd alloys containing Zn [J]. Scripta Materialia, 2005, 53(9): 1049−l053.

[2] H E S M, ZENG X Q, PENG L M, GAO X, NIE J F, DING W J. Microstructure and strengthening mechanism of high strength, Mg-10Gd-2Y-0.5Zr alloy [J]. Journal of Alloys and Compounds, 2007, 427(1): 316−323.

[3] WANG W, WU G H, WANG Q D, HUANG Y G, DING W J. Gd contents, mechanical and corrosion properties of Mg-10Gd-3Y-0.5Zr alloy purified by fluxes containing $GdCl_3$ additions [J]. Materials Science and Engineering A, 2010, 527(6): 1510−1515.

[4] AFSHAR M R, ABOUTALEBI M R, ISAC M, GUTHRIE R I L. Mathematical modeling of electromagnetic separation of inclusions from magnesium melt in a rectangular channel [J]. Materials Letters, 2007, 61(10): 2045−2049.

[5] AFSHAR M R, ABOUTALEBI M R, GUTHRIE R I L, ISAC M. Modeling of electromagnetic separation of inclusions from molten metals [J]. International Journal of Mechanical Sciences, 2010, 52(9): 1107−1114.

[6] AHMAD A, PURBOLAKSONO J, YAHYA Z. Estimating inclusion size in WE43-T6 magnesium alloys based on Gumbel extreme values [J]. Materials Science and Engineering A, 2009, 513−514: 319−324.

[7] SARA L. Estimating inclusion distributions of hard metal using fatigue tests [J]. International Journal of Fatigue, 2003, 25(2): 129−137.

[8] HASHIMOTO A, MIYAZAKI T, KANG H G, NOGUCHI H, OGI K. Estimation of particle size distribution in materials in the case of spheroidal particles using quantitative microscopy [J]. Journal of Testing and Evaluation 2000, 28(5): 367−377.

[9] HAERLE A G, MIKUCKI B A, MERCER W. A new technique for quantifying non-metallic inclusion content in magnesium [J]. Light Metal Age (USA). 1996, 54(7−8): 22−24, 26, 28−29.

[10] GAO Hong-tao, WU Guo-hua, DING Wen-jiang, ZHU Yan-ping. Purifying effect of new flux on magnesium alloy [J]. Transaction of Nonferrous Metals Society of China, 2004, 14(3): 530−536.

[11] ZHANG Jun, HE Liang-ju, LI Pei-jie. Purification technique of regenerated magnesium alloy melt [J]. Foundry, 2005, 54(7): 665−669. (in Chinese)
[12] ZHANG Shi-hang, WEI Bo-kang, LIN Han-tong. Investigation on MgO inclusions and refining mechanism of magnesium alloy [J]. Foundry, 2003, 52(7): 488−491. (in Chinese)
[13] ZHAO Y, LIU P P, ZHOU H. Inclusions of AZ91D magnesium alloy [J]. Foundry Technology, 2006, 27(8): 834−838. (in Chinese)
[14] WANG W, HUANG Y G, WU G H, WANG Q D, SUN M, DING W J. Influence of flux containing YCl_3 additions on purifying effectiveness and properties of Mg-10Gd-3Y-0.5Zr alloy [J]. Journal of Alloys and Compounds, 2009, 480(2): 386−391.
[15] CHANG J W, FU P H, GUO X W, PENG L M, DING W J. Effect of heat treatment on corrosion and electrochemical behaviors of Mg-3Nd-0.2 Zn (wt.%) magnesium alloy [J]. Electrochimica Acta, 2007, 52(9): 3160−3167.

夹杂物对GW103K镁合金服役性能的影响

梁敏洁[1,2], 吴国华[1], 丁文江[1], 王 玮[1]

1. 上海交通大学 材料科学与工程学院，上海 200240；2. 中北大学 材料科学与工程学院，太原 030051

摘 要：研究未净化、MgO陶瓷过滤及JDMJ熔剂净化等净化条件下，夹杂物对GW103K(Mg-10Gd-3Y)合金微观组织、力学性能和腐蚀性能的影响。结果表明：采用JDMJ熔剂净化后的GW103K合金，夹杂物的数量和尺寸明显减少，其抗拉强度和伸长率增加，而屈服强度则低于使用MgO陶瓷过滤净化和未经净化的合金。此外，随着夹杂物含量的减少，合金的腐蚀速率从2.419 mg/(cm^2·d) 快速下降到1.265 mg/(cm^2·d)，当夹杂物含量(体积分数)达到0.385%后，合金的腐蚀速率几乎不再发生变化。建立不同净化条件下夹杂物的体积分数和GW103K合金服役性能的内在联系。

关键词：Mg-10Gd-3Y合金；夹杂物；净化；服役性能

(Edited by LI Xiang-qun)